

# PIONIER: A Four-telescope Instrument for the VLTI

G rard Zins<sup>1</sup>  
 Bernard Lazareff<sup>1</sup>  
 Jean-Philippe Berger<sup>2</sup>  
 Jean-Baptiste Le Bouquin<sup>1</sup>  
 Laurent Jocou<sup>1</sup>  
 Sylvain Rochat<sup>1</sup>  
 Pierre Haguenaue<sup>2</sup>  
 Jens Knudstrup<sup>2</sup>  
 Jean-Louis Lizon<sup>2</sup>  
 Rafael Millan-Gabet<sup>3</sup>  
 Wes Traub<sup>4</sup>  
 Myriam Benisty<sup>5</sup>  
 Alain Delboulbe<sup>1</sup>  
 Philippe Feautrier<sup>1</sup>  
 David Gillier<sup>1</sup>  
 Philippe Gitton<sup>2</sup>  
 Pierre Kern<sup>1</sup>  
 Mario Kiekebusch<sup>2</sup>  
 Pierre Labeye<sup>6</sup>  
 Didier Maurel<sup>1</sup>  
 Yves Magnard<sup>1</sup>  
 Mickael Micallet<sup>1</sup>  
 Laurence Michaud<sup>1</sup>  
 Thibaut Moulin<sup>1</sup>  
 Dan Popovic<sup>2</sup>  
 Alain Roux<sup>1</sup>  
 Noel Ventura<sup>1</sup>

<sup>1</sup> Institut de Plan tologie et d'Astrophysique de Grenoble (IPAG), OSUG, Universit  Joseph Fourier, Grenoble, France

<sup>2</sup> ESO

<sup>3</sup> NASA Exoplanet Science Institute, California Institute of Technology, Pasadena, USA

<sup>4</sup> Exoplanet Exploration Program, Jet Propulsion Laboratory, Pasadena, USA

<sup>5</sup> Max-Planck-Institut f r Astronomie, Heidelberg, Germany

<sup>6</sup> Laboratoire d'Electronique et Technologies de l'Information (LETI), Grenoble, France

PIONIER, developed by the Institut d'Astrophysique de Grenoble (IPAG) and installed at the VLT Interferometer, is a near-infrared (1.5–2.4  $\mu\text{m}$ ) instrument that allows the beams from four telescopes to be recombined for the first time, thus permitting high angular resolution imaging studies at an unprecedented level of sensitivity and precision. At the heart of the instrument is an integrated optics beam combiner (IOBC) that splits and recombines the four incoming signals, provid-

ing excellent compactness and stability. The IOBC has been developed by IPAG and the Laboratoire d'Electronique et Technologies de l'Information. PIONIER was successfully commissioned in October 2010, 12 months after being approved by ESO as a visitor instrument. With the baselines up to 130 metres offered by the VLTI, PIONIER can resolve structures less than 3 milliarcseconds across. The scientific motivation behind PIONIER is outlined, the instrument is described and illustrative scientific results from the first year of operation are presented.

## Introduction

Since October 2010, the visitor instrument PIONIER has been recombining the light of all four beams of the Very Large Telescope Interferometer (VLTI), enabling new science at the highest angular resolution.

Infrared interferometry has been one of the baseline goals for the Paranal Observatory since its inception. Major milestones have been the first fringes between VLT Unit Telescopes (UTs) in March 2001, and the first fringes between the Auxiliary Telescopes (ATs) in February 2005. The VLTI infrastructure is currently structured for four telescopes. The AMBER instrument (commissioned in 2004) allows three-telescope operation, leaving the full potential of the VLTI yet to be realised.

For about the last ten years, the Laboratoire d'Astrophysique de l'Observatoire de Grenoble (LAOG), now merged into the Institut d'Astrophysique de Grenoble (IPAG<sup>1</sup>) and the Laboratoire d'Electronique et Technologies de l'Information (LETI<sup>2</sup>), has been developing integrated optics components for infrared interferometry. One outcome of this effort was a four-beam *H*-band combiner. This integrated combiner opened an opportunity for the PIONIER instrument, which has been designed to exploit the full potential of the VLTI array in preparation for the arrival of the second generation instruments GRAVITY (see Eisenhauer et al., 2011) and MATISSE (Hofmann et al., 2008). The main observational motivation is the possibility of using four telescopes simultaneously, which provides six visibilities and three independent closure phases per

wavelength channel and one closure amplitude, whereas a three-telescope combiner only provides three visibilities and one closure phase. The remarkable success of the four-telescope (4T) CHARA interferometer (Monnier et al., 2007) has demonstrated that such an increase in *uv*-plane coverage significantly improves the capability to reconstruct a "model-independent" image from the observables, so-called aperture synthesis imaging.

In November 2009, PIONIER was approved as a visitor instrument by the ESO Scientific and Technical Committee. Less than twelve months later, the completed instrument was brought to Paranal; see ESO Announcement 1081<sup>3</sup>.

## Scientific motivation

The initial core science goals of PIONIER were to provide spatially resolved diagnostics, at the level of 1 astronomical unit (AU), for the close environments of planet-forming stars. This capability will place direct constraints on the physical conditions at the distances from the star where planets may form. The PIONIER target list spans different evolutionary stages of planet-forming environments around stars of different masses. The dusty environments of massive and intermediate-mass (Herbig AeBe) young stars are ideal candidates for aperture synthesis since their angular extent is of the order of 10 milliarcseconds (mas). The direct or modelled images provide unique diagnostics to constrain the structure of the inner rim of their protoplanetary discs. Of particular importance is the possibility of obtaining direct images of the morphology of the dust/gas inner disc rim (and in particular its vertical structure and possible clumpiness), and of studying the dust's properties and the role of extended scattering envelopes in the global radiative energy balance.

PIONIER's sensitivity allows the "T Tauri barrier" to be broken and opens the way to direct spatially resolved observation of young solar analogues that have demanded more sensitivity than currently available for VLTI near-infrared (NIR) observations until now. T Tauri stars with discs at different evolutionary stages

are a focus of PIONIER observations, with a particular emphasis on obtaining direct diagnostics of the presence of planet-forming signatures, such as huge gaps in the emission. PIONIER observations have proved to be remarkably complementary to constraints provided by advanced disc-modelling using Spitzer and Herschel data, since they allow an unambiguous constraint on the inner disc boundary and radial emission. Furthermore PIONIER aims at reaching a closure phase accuracy sufficient to hunt down stellar, substellar and maybe hot planetary companions and to contribute to the statistical study of multiplicity in planet-forming environments. In a similar vein, PIONIER is designed to push visibility precision to a level where it can reveal the hot dust component that has been recently pinpointed around debris-disc host stars (e.g., Absil et al., 2009).

The sensitivity and mapping capability of PIONIER also opens new territories requiring milliarsecond direct or parametric mapping, such as for interacting binaries, stellar surfaces, Wolf-Rayet stars, etc.

### System overview

Each of the beams from the VLTI switchyard first enters the injection and optical path delay unit (IOPDU, see Figure 1), where the *H*-band light is reflected from a dichroic mirror, while the *K*-band light is transmitted to the VLTI infrared image sensor (IRIS) guiding camera. The roles of the *H*- and *K*-bands can be exchanged in a planned extension to *K*-band observation. The following elements on the signal path are a flat mirror on a piezo stage with a 400  $\mu\text{m}$  travel, a piezo tip-tilt mirror with a bandwidth of 100 Hz and a throw of  $\pm 200$  arcseconds that responds to input from IRIS, a shutter, a birefringence compensation plate, and an off-axis parabola for injection into an optical fibre. Other elements, not on the signal path, are used for alignment or spectral calibration.

The integrated optics beam combiner (see Figures 2 and 3) takes the four input signals and delivers 12 outputs (24 for the ABCD variant): six baselines times two phase states:  $a + b$  and  $a - b$ . The

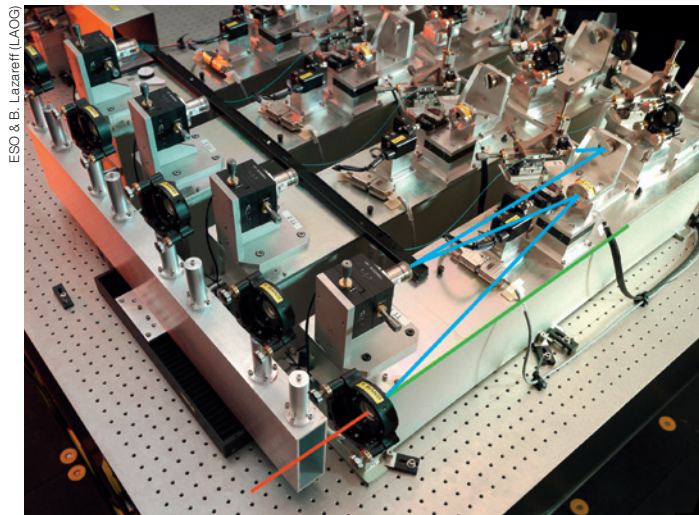


Figure 1. Partial view of the PIONIER IOPDU. The beam from the VLTI switchyard is split by a dichroic plate. The *K*-band is transmitted to the IRIS guiding camera, while the *H*-band beam (blue line) is reflected and follows the path: OPD piezo (used to modulate the optical path and scan the fringes), tip-tilt stage (used to track the focal plane position of the target), birefringence compensation plate, and finally an off-axis parabola for injection into the optical fibre, on its way to the beam combiner.

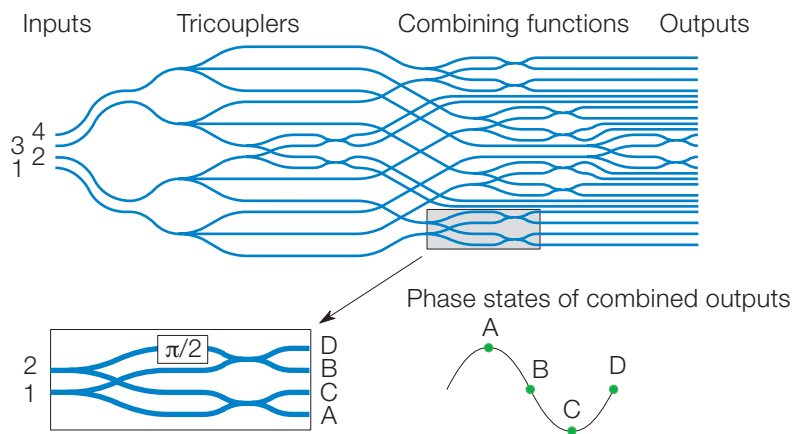


Figure 2. Top: schematic of a 4T-ABCD combiner. Each input is divided in three to interfere with other inputs in an elementary combining block. Bottom left: detail of one combining block. Each input is further divided in two; after a  $\pi/2$  phase shift is applied in one arm, pairwise combinations are made in

couplers. Bottom right: representation of the four (relative) phases achieved in the four outputs. In a simplified version, called 4T-AC, the Y-junction and  $\pi/2$  phase shift are omitted; so each pairwise combiner has only two outputs instead of four.

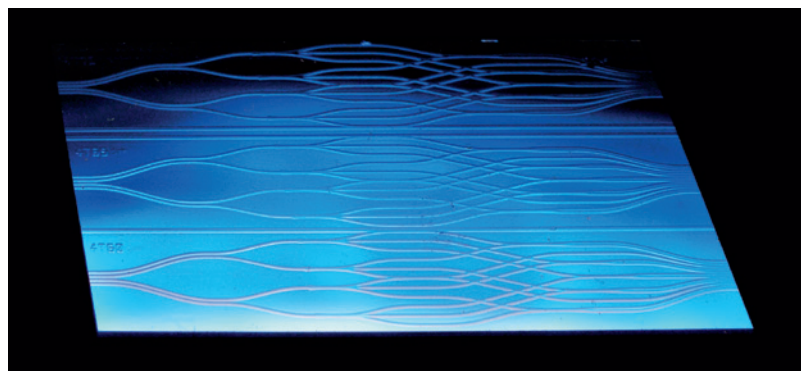


Figure 3. Picture of a 4T-AC integrated optics beam combiner. The buried optical waveguides are revealed by small deviations from surface flatness,

amplified by the specular lighting. Beam propagation is left to right.

outputs of the IOBC are imaged by 1:1 relay optics onto the detector; a dispersing prism and/or a Wollaston polarisation separator can also be inserted. Two available prisms can disperse the  $H$ -band over 7 pixels (for spectral resolution  $R \sim 40$ ) or three pixels (for  $R \sim 20$ ).

The detector is a  $128 \times 128$  Rockwell PICNIC in a commercial liquid nitrogen cryostat, both kindly on loan from JPL. After amplification and 16-bit numerical conversion, the signal is acquired by the detector control system (DCS).

### Integrated optics combiner

The interferometric combination is achieved in a thumb-sized integrated optics element. This silica-on-silicon chip embeds a single-mode optical circuit capable of combining four beams in a pair-wise scheme. There are four main drivers for this choice: 1) single-mode spatial filtering associated to proper photometric monitoring provides significant improvements in the accuracy of the observables; 2) the extreme compactness of the chip ensures excellent stability of the instrument response; 3) the complex circuit is permanently aligned and only requires the adjustment of the light injection and the output on the detector (unlike discrete component optics); 4) different designs can be swapped and tested with minimal realignment.

The basic design is described in detail in Labeye et al. (2006), Labeye (2009) and Benisty et al. (2009). The four incoming beams are each split into three and rearranged in six pairs. For each pair (baseline), a “static-ABCD” combining cell is implemented. It generates four phase states simultaneously (nominally in quadrature), for a total of 24 outputs. This combiner can be used both in fringe-scanning mode (VINCI-like) or ABCD-like mode (PRIMA-like). Such combiners have been developed for the  $H$ -band and for the  $K$ -band (Jocou et al., 2010). These are the most complex interferometric circuits ever used on-sky.

To increase the signal-to-noise and the readout speed in fringe-scanning mode, a variant has been designed using only the A and C outputs ( $\pi$  phase difference);

that variant (AC) is currently in operation. The combiner is fed by polarisation-maintaining single-mode  $H$ -band fibres, whose lengths have been equalised with an accuracy of  $20 \mu\text{m}$ , so that they introduce a negligible differential chromatic dispersion.

### Polarisation control

A collateral effect of using polarisation-maintaining fibres to carry the signal from the injection unit to the integrated combiner is that such fibres are strongly birefringent, accumulating a phase difference between their principal axes at a rate of one turn every few millimetres. Even if the lengths of the fibres are carefully matched, and they are taken from the same fabrication batch, their birefringence will not match to a fraction of a wavelength. The differential optical path difference (OPD) between fringes in orthogonal polarisations was measured and found typically to be a few wavelengths. In the initial design, the two linear polarisations were spatially separated by a Wollaston prism, and detected separately. This approach of course carries penalties in both signal-to-noise and readout speed.

It was decided to insert a birefringent plate into the signal path between the tip-tilt mirror and the injection parabola (see Figure 1). This plate is made from lithium niobate, a uniaxial material that has good transmission in the  $H$ - and  $K$ -bands. Each plate is  $X$ -cut, i.e. the extraordinary axis is in the plane of the plate. Without going into detailed calculations, it is apparent that:

- (a) When the plate is perpendicular to the beam, it introduces a differential OPD between the two polarisations, which is the product of the plate thickness and the difference of refractive indices for the ordinary and extraordinary rays ( $n_o - n_e$ );
- (b) If the plate is tilted, for example about the  $n_o$  axis, the two polarisations will follow different geometrical paths and experience different optical indices, with a net differential OPD that depends upon the inclination.

Lithium niobate is a suitable material for this application because its birefringence

( $n_o - n_e$ ) =  $-0.073$  is large enough at  $1.6 \mu\text{m}$ , with only a small wavelength dependence (a quality not shared by quartz). The compensation plates are  $2 \text{ mm}$  thick and tilted typically by  $20^\circ$ . In practice, the Wollaston is inserted, then the inclination of the plates is adjusted so that both the wavepacket envelopes and the individual fringes coincide between the two polarisations on each of the six baselines. The Wollaston is removed for all observations, and the co-aligned fringes from both polarisations are detected jointly on the same detector pixel.

### Camera and readout electronics

The scientific requirements for the camera are low noise (faint targets), high speed (atmospheric phase coherence time typically a few milliseconds) and large dynamic range. Our implementation strives to meet these requirements as far as the intrinsic parameters of the detector allow.

The PICNIC detector has a spectral response extending from  $850 \text{ nm}$  to  $2500 \text{ nm}$ , with a quantum efficiency of  $60\text{--}65\%$ . Two filter wheels are located inside the cryostat. The first one defines the bandpass:  $H$ -band ( $1.5\text{--}1.82 \mu\text{m}$ ) or  $K$ -band ( $2.0\text{--}2.36 \mu\text{m}$ ). The second wheel, generally in the “open” position, carries neutral density (ND) filters for  $\text{ND} = 0.6$ ,  $\text{ND} = 1.4$ , and  $\text{ND} = 2.0$  that are inserted when observing bright objects. The PICNIC detector has the interesting property of non-destructive readout: it is possible to perform sequentially partial integrations without an intervening reset. See the section “Observing modes”.

A differential amplifier (gain  $\times 10$ ) inside the cryostat provides a good immunity against common-mode electrical perturbations. Differential signal wiring is preserved up to the inputs of a fast ( $250 \text{ ns}$ ) 16-bit analogue-to-digital (A/D) converter in the warm electronics. The patterns for the various timing and housekeeping signals of the detector (line, pixel, reset, etc...) are updated at a clock rate of  $5 \text{ MHz}$ , which provides reasonably fine-grained control of the timing.

The minimum detector readout time per pixel (typically  $6 \mu\text{s}$ ) is set by the intrinsic time constant of the PICNIC array. Repeating A/D conversions (duration  $0.25 \mu\text{s}$ ) on the same pixel up to eight times, reduces the readout noise. Detection gain and noise of the detector were characterised by the standard mean–variance method. In essence, the detector gain, expressed in A/D units (ADU) per electron can be calibrated exploiting the known statistics of electron counts: variance = mean. Table 1 summarises the detector characteristics.

Parameter	Value (median)
Gain ADU/e <sup>-</sup>	0.26
Readout noise e <sup>-</sup>	18.5 (a)
Readout noise e <sup>-</sup>	15.2 (b)

**Table 1.** Measured electronic gain and readout noise of the PICNIC detector. Two values are given for the readout noise: (a) for zero illumination, but including the variance of the dark current; (b) excluding the contribution from the dark current.

### Instrument control

Although PIONIER is a visitor instrument, the control software is fully compliant with the ESO VLT standards, and consists of standard components such as observation software (OS), instrument control software (ICS) and detector control software (DCS). This compliance allows full interoperability with all sub-systems of the VLT, enabling rapid installation at the telescope site and easing the operations of the instrument. PIONIER is thus operated at Paranal as other VLT instruments.

However, PIONIER introduces several interesting innovations:

**Programmable logical controller (PLC) for the ICS** — Due to constraints on the project, such as a tight budget, space requirements and thermal dissipation, it was decided to use an embedded programmable controller (PC) from the company Beckhoff instead of traditional VME-based local controller units (LCUs) running VxWorks. This computer is an industrial PLC, controlling distributed input/output components through the EtherCAT fieldbus. The VLT software has been extended to support fieldbus technology (IC0 fieldbus extension). Device drivers have been developed to control



**Figure 4.** Part of the PIONIER/VLTI team taking a break during the instrument commissioning.

the instrument functions like stepper motors, lamps, shutters and sensors via EtherCAT terminals (Kiekebusch et al., 2010).

**DCS** — The detector front-end and video electronics used in PIONIER are not the standard system, normally provided by ESO. Therefore it has been necessary to re-implement the software controlling the detector. This software is a multi-threaded application whose design is inspired from the new generation controller (NGC) DCS, developed by ESO. The customised DCS implemented for PIONIER is compatible with the NGC interface, to make integration with the OS transparent. This application is in charge of driving the detector by generating the clock patterns for the different readout modes (simple, double and Fowler sampling), to acquire detector data and drive the piezo to synchronise OPD modulation with detector readout cycles. It is also in charge of pro-

cessing and delivering detector data to all clients requiring this, such as the real-time display (RTD) or the alignment control software (ACS; see below).

**ACS** — A dedicated software component, called the alignment control software, has been implemented to perform alignment tasks. This consists of: 1) optimising the flux injection into fibres by creating a map of fluxes and fitting a Gaussian to find the maximum; and 2) performing fast guiding to compensate for turbulence using positional errors delivered by IRIS through the reflective memory network (RMN). This software runs on the detector LCU for fast communication with the DCS. In this way, it is possible to perform flux injection optimisation in a very efficient way; less than 20 seconds per beam is achievable in most cases.

**RTD scope** — In fringe-scanning mode, the RTD scope application retrieves data from the DCS for each scan sequence, displays it to the user and computes the OPD which is forwarded back to the DCS

for group delay tracking. This application, running on the instrument workstation, has been implemented by PIONIER scientists using the Yorick tool, which provides advanced functions for data processing and display.

**Ethernet-based controllers** — The controllers for the piezo and for the tip-tilt devices, are the E-712 and E-517 digital controller modules from the company Physik Instrumente. These are driven through transmission control protocol/internet protocol (TCP/IP) interfaces. This solution offers more flexibility than the analogue interface normally used. The devices can be controlled from any system that has an Ethernet interface and there is no cable length limitation between the controller and the driving system, which is the DCS. PIONIER performance tests have been done up to 2 kHz with good results with this system.

### Observing modes

Almost all observations are made in the so-called Fowler mode. Following a reset of the detector, a series of  $N_{read}+1$  readouts are performed (at the maximum rate performed by the detector and electronics), defining  $N_{read}$  consecutive integration periods. This sequence takes typically a few hundred milliseconds. The base value of  $N_{read}$  is 512, under fair to good atmospheric conditions. For sources weaker than  $H = 6$  mag,  $N_{read}$  is increased (more integration time per fringe), Simultaneous with the readouts, the piezo stages are scanned following a linear ramp, with respective throws  $-3A$ ,  $-A$ ,  $+A$ ,  $+3A$ , so that the OPD for any baseline is swept over an amplitude of  $2A$ ,  $4A$ , or  $6A$ . The default value is  $A = 40 \mu\text{m}$ .

For very bright sources ( $H < 0$  mag), when the minimum time for a Fowler scan would saturate the detector, a series of separate reset-read-read sequences are performed during the piezo scan, with an extra overhead from the extra reset and read operations. For each integration period, the number of pixel detectors acquired is 12 or 24 (number of IOBC outputs) times the number of spectral channels: 1 (no dispersion), 3 (lower resolution prism) or 7 (larger resolution prism). Table 2 lists the time per scan in various

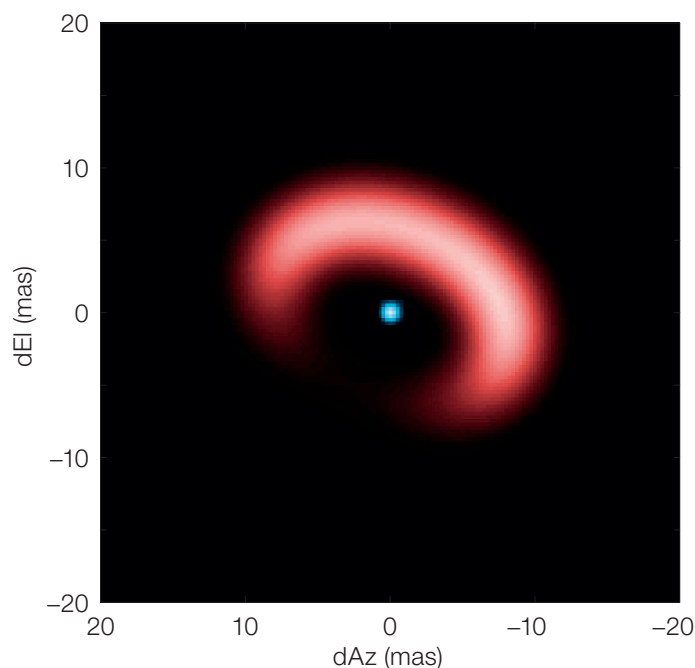


**Figure 5.** A parametric model reconstruction of the circumstellar environment of the Be star HD45677. The different “colours” of the star and circumstellar matter pose a challenge to existing image reconstruction techniques; a simple parametric model gives a reasonable fit to the observed visibilities and closures. The ring-shaped emission in the  $H$ -band is thought to originate at the inner boundary of the circumstellar disc, where the intense radiation of the star causes the sublimation of interstellar dust grains.

configurations with the currently used AC beam combiner. The actual elapsed time may be longer due to overheads, e.g., evaluation of wave packet position.

$N_{read}$	$N_s$	$N_{disp}$	$t(ms)$
512	1	1	126
512	1	7	383
2048	1	1	294
2048	8	1	366

**Table 2.** Duration of one scan, in various configurations.  $N_{read}$  is the number of readouts in one scan;  $N_s$  is the number of repeated A/D conversions for one pixel;  $N_{disp}$  is number of wavelength channels, when a dispersing prism is used.

### Integrated data flow

Although it is a visitor instrument, PIONIER follows the ESO data flow as far as possible. From the high-level point of view, PIONIER is operated via the broker of observing blocks (BOB) that executes observing blocks (OBs) fetched from the standard P2PP ESO software. OBs can be conveniently generated by the ASPRO2<sup>4</sup> preparation software from the Jean-Marie Mariotti Center (JMMC). This tool automatically fetches the target coordinates, proper motions, magnitudes and other parameters from the Centre de Données Stellaires (CDS) database. This saves time and avoids typing errors.

The PIONIER data reduction software is publicly available<sup>5</sup> as a YORICK package; see Le Bouquin et al. (2011) for more information. It converts the raw FITS file produced by the instrument into calibrated visibilities and closure phases written in the standard OIFITS format. Angular diameters of calibration stars are automatically recovered from published catalogues. Consequently, the final products are science-ready and can be directly handed over to software such as LITpro<sup>6</sup> (model fitting) or MIRA<sup>7</sup> (image reconstruction).

The PIONIER data reduction software runs in the background during the night. The science-ready outputs are available about 30 minutes after the beginning of the observations, once the first calibration star has been observed. This allows the data quality to be assessed and decisions are taken accordingly. This is also a powerful tool to quickly identify bad calibration stars, such as previously unknown binaries, and re-execute an additional calibration. Finally, we were sometimes able to obtain an image reconstruction of the observed target even before the end of the night.

To optimise the scientific return of PIONIER in the medium term, we maintain a simple archive at IPAG, which

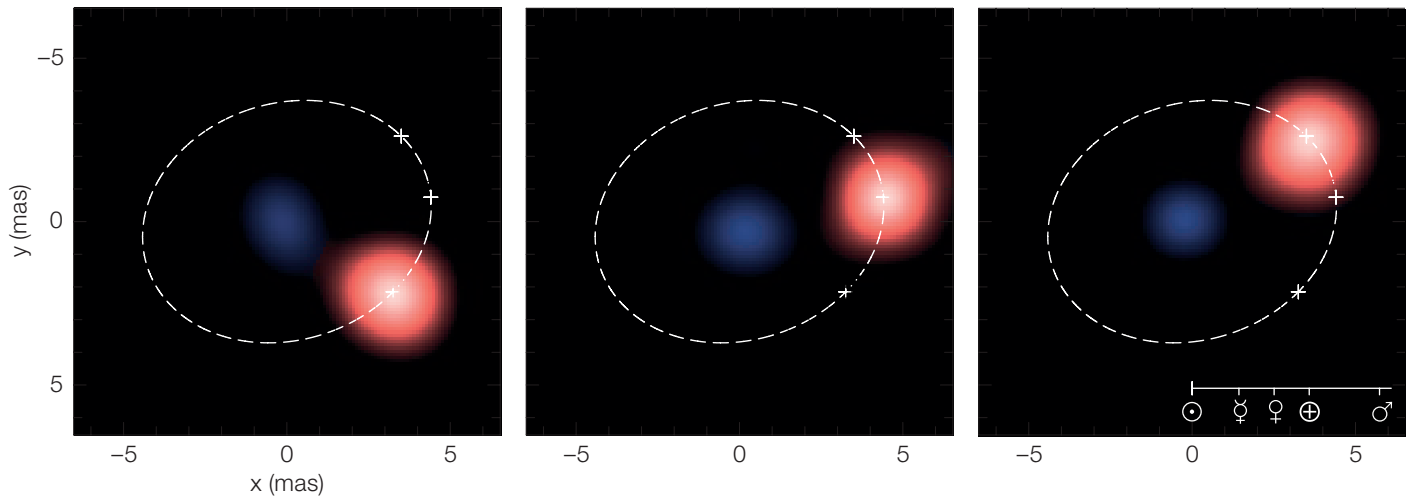


Figure 6. Multi-epoch image reconstructions of the symbiotic binary SS Lep (see Blind et al. 2011 and ESO release 1148). The system is composed of a cool red giant in orbit around a hot blue dwarf with a period of 235 days. The stars are so close that several episodes of mass transfer occurred in the recent past of the system, explaining the so called “Algol paradox”, where the most massive component (A dwarf) is also the least evolved. The size of the inner Solar System is shown for reference.

includes both the raw FITS files and the science-ready OIFITS products.

### PIONIER results

Capitalising on previous developments and available experience, PIONIER was built in about one year, providing the capability to recombine all four VLTI beams for the first time. First fringes on-

sky were obtained five days after we started unpacking the transport boxes and two hours after the instrument received the VLTI beams. A number of scientific programmes have been executed during the first year of operation; examples of results are shown in Figures 5 and 6. PIONIER not only bridges the gap to VLTI second generation instruments, but may also serve as a testbed for certain aspects of these instruments.

### References

Abil, O. et al. 2009, ApJ, 704, 150  
 Benisty, M. et al. 2009, A&A, 498, 601  
 Blind, N. et al. 2011, A&A, 536, A55  
 Eisenhauer, F. et al. 2011, The Messenger, 143, 16  
 Jocou, L. et al. 2010, Proc. SPIE, Volume 7734  
 Hofmann, K.-H. et al. 2008, SPIE, 7013, 122

Labeye, P. et al. 2006, in Silicon Photonics, Proc. SPIE, 6125, 161  
 Labeye, P. 2009, PhD dissertation, INPG, <http://arxiv.org/abs/0904.3030>  
 Le Bouquin, J.-B. et al. 2011, A&A, 535, A67  
 Monnier, J. D. et al. 2007, Science, 317, 342

### Links

- <sup>1</sup> Institut de Planétologie et d’Astrophysique de Grenoble (IPAG): <http://ipag.obs.ujf-grenoble.fr/>
- <sup>2</sup> Laboratoire d’Electronique et Technologies de l’Information (LETI): <http://www-leti.cea.fr/>
- <sup>3</sup> ESO announcement 1081: <http://www.eso.org/public/announcements/ann1081/>
- <sup>4</sup> ASPRO2 preparation software: [http://www.jmmc.fr/aspro\\_page](http://www.jmmc.fr/aspro_page)
- <sup>5</sup> PIONIER data reduction software: <http://apps.jmmc.fr/~swmgr/pndrs>
- <sup>6</sup> LITpro model fitting software: <http://www.jmmc.fr/litpro>
- <sup>7</sup> MIRA image reconstruction software: <http://www-obs.univ-lyon1.fr/labo/perso/eric.thiebaut/mira.html>



Panoramic view of the Very Large Telescope Interferometer (VLTI) tunnel, showing two delay lines.